



OPEN

SUBJECT AREAS:

SYNTHESIS AND
PROCESSINGMECHANICAL AND STRUCTURAL
PROPERTIES AND DEVICESStrengthening of Graphene Aerogels
with Tunable Density and High
Adsorption Capacity towards Pb^{2+} Zhuo Han^{1,2}, Zhihong Tang¹, Shuling Shen¹, Bin Zhao¹, Guangping Zheng^{1,2} & Junhe Yang¹Received
15 January 2014Accepted
6 May 2014Published
22 May 2014

Correspondence and
requests for materials
should be addressed to
Z.H.T. (zhtang@usst.
edu.cn) or J.H.Y.
(jhyang@usst.edu.cn)

¹School of Materials Science and Engineering, University of Shanghai for Science and Technology, Shanghai 200093, China,²Department of Mechanical Engineering and Shenzhen Research Institute, Hong Kong Polytechnic University, Hung Hom, Kowloon, Hong Kong, China.

Graphene aerogels (GAs) with high mechanical strength, tunable density and volume have been prepared only via soaking graphene hydrogels (GHs) in ammonia solution. The density and volume of the obtained GAs are controlled by adjusting the concentration of ammonia solution. Although volume of the GAs decreases with increasing the concentration of ammonia solution, its specific surface area maintains at about $350 \text{ m}^2 \text{ g}^{-1}$, and the inner structure changes to radial after ammonia solution treatment. Thus, GAs are particularly suitable for the adsorption and energy storage applications owing to their high specific surface area and unique porous structure. The adsorption capacity of GAs for Pb^{2+} from aqueous solution maintains at about 80 mg g^{-1} , which could reach as high as 5000 g m^{-3} per unit volume and they can be separated easily from water after adsorption.

Graphene or functionalized graphene has provided numerous possibilities for applications in many fields because of its superior physical and chemical properties^{1–3}. The assembly of graphene into three-dimensional (3D) macroscopic structures has attracted much attention⁴ since it paves a way to implement the superior properties of individual graphene sheets for macroscopic applications, such as energy storage^{5,6}, bionics research^{7–9}, water treatment^{10,11} and template frame^{12,13}. Usually these applications require well-defined structures with high mechanical strength as well as high porosity. In the past several years, much effort had been devoted to the fabrication of monolithic graphene based solid structures with high porosity, including in-situ self-assembly^{14,15}, hydrothermal method¹⁶, molecular templates¹⁷, Langmuir–Blodgett assembly¹⁸, layer-by-layer assembly¹⁹, and direct chemical vapour deposition on selected substrates^{20–22}. Among those advanced fabrication methods, hydrothermal method is the most attractive one due to its low cost and easy implementation.

Graphene aerogel (GA), a nanoscaled graphene aggregation network with low density, large open pores and high specific surface area, is usually prepared from graphene oxide via hydrothermal method and subsequent supercritical fluid drying or freeze drying. However, the high porosity of GAs usually sacrifices their mechanical strength, which will prevent them from wide-spread applications^{23–25}. Hence graphene aerogel with improved mechanical performance is urgently needed.

Recently, the preparation of 3D graphene is of great interest. Tang et al. prepared noble-metal promoted graphene aerogel, which had a compressive strength of 0.042 MPa and exhibited excellent catalysis performance²⁶; 3D nitrogen riched GA with uniformly-distributed Pt/Ru nano particles was also prepared, which demonstrated good performance for methanol electrochemical oxidation reaction²⁷; Gao et al. obtained polydopamine-modified graphene hydrogel (PDA-GH) via one-step hydrothermal method, and demonstrated its high adsorption capacity towards heavy metals, synthetic dyes, and aromatic pollutants¹¹; Sun and co-workers fabricated all carbon ultra-flyweight aerogels (UFAs with density $\rho \geq 0.16 \text{ mg cm}^{-3}$) with high adsorption capability for CCl_4 from freeze-drying aqueous solutions of carbon nanotubes (CNTs) and graphene oxide (GO)²⁵. Hu et al. also prepared ultralight graphene aerogels functionalized by ethylenediamine²³. Cong et al. reported a one-step fabrication of macroscopic multifunctional graphene-based hydrogels by adding ferrous ions and in situ simultaneous deposition of nanoparticles on graphene sheets, which exhibited excellent performance in the removals of pollutants²⁸; Similar researches were carried out by other groups through modifying graphene oxide by polymers^{29,30}, metal nanoparticles^{6,10} and metal ions^{31,32}. Although progresses had been made in the preparation and application of GAs or functionalized GAs, the application of which was still restricted by their relative low mechanical strength and easy dispersion in polar solvent because of their abundant oxygen functional groups. It is

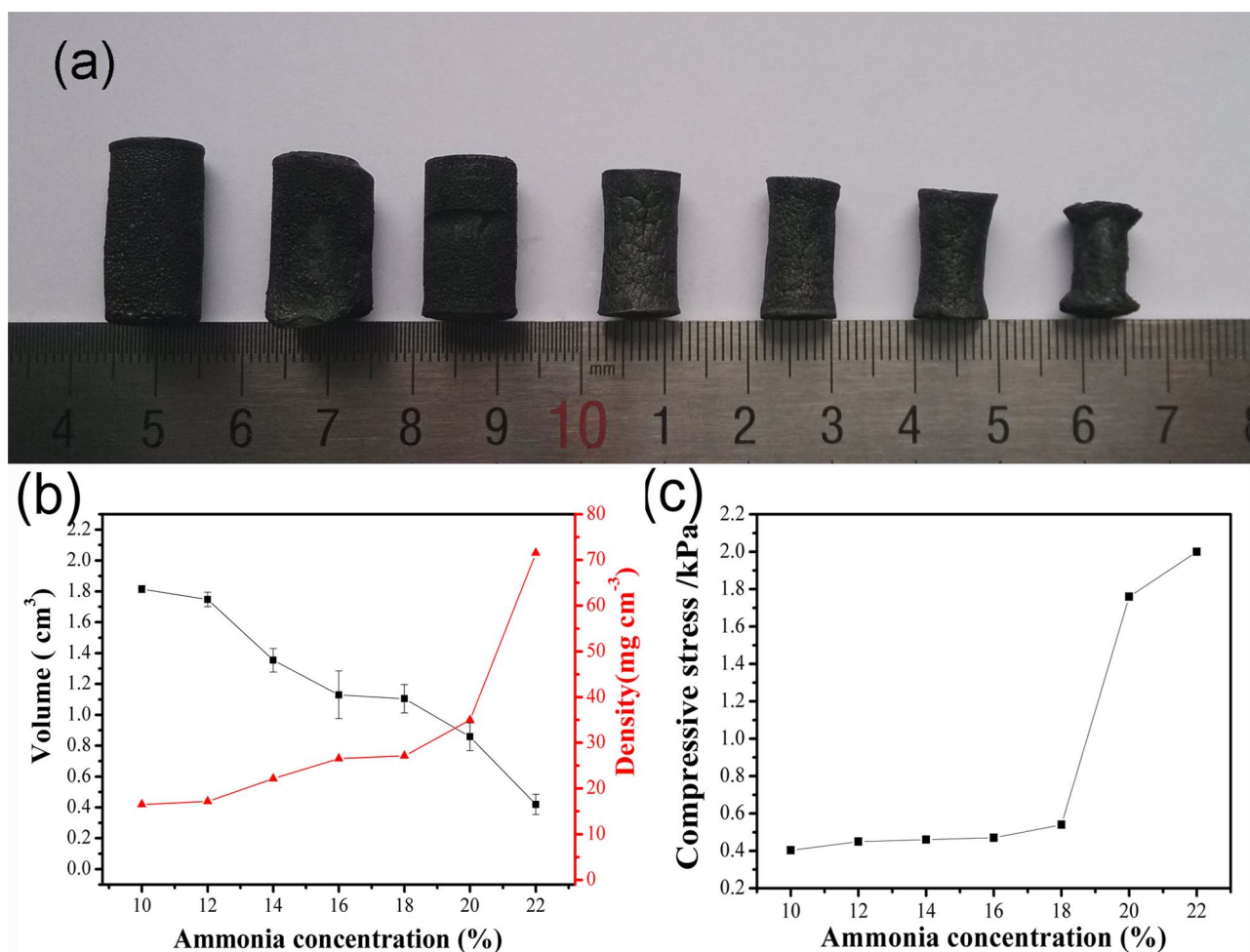


Figure 1 | (a) Photographs of a-GA-10%, a-GA-12%, a-GA-14%, a-GA-16%, a-GA-18%, a-GA-20% and a-GA-22% with the same mass and different volumes (from left to right). (b) The volumes of a-GA-N and their corresponding densities. (c) The compressive strengths of a-GA-N samples.

noted that in the hydrothermal fabrication methods, the volume and density of the GA were only controlled by the size of the container or the concentration of graphene oxide solution, which cannot be fully controlled. Therefore, how to control the microstructural characteristics of GAs such as density and porosity in a flexible manner is still one of the challenging issues that hinder the development of next generation GA based materials.

Herein, GAs with high mechanical strength and tunable volume or density are prepared by simply soaking the GHs in ammonia solution. Volume or density of GAs is controlled by the controllable shrinkage of GHs during freeze drying, and which is adjusted by the concentration of ammonia solution. The improved mechanical strength is associated with the shrinkage of GA, which is increased to 2.1 kPa when the density of GA increases to 70 mg cm^{-3} (the volume is reduced to 33% of that before treatment). Remarkably, the samples demonstrate excellent adsorption ability for Pb^{2+} and organic solvents in spite of the volume shrinkage. In addition, the sample can be easily removed from the solvent after adsorption processes, indicating its great potential in the practical applications as environmental friendly materials.

Results and discussion

In our previous study, strengthened 3D GA was obtained by pre-treating graphene hydrogel (GH) in ammonia solution³³. The present work demonstrates that besides the enhancement of mechanical strength, the volume and density of GAs can be controlled easily by adjusting the concentration of ammonia solution. Figure 1(a)

clearly shows that the volume of the GAs decreases gradually when they are treated by the ammonia solution with increasing the concentration, and which decreases significantly when the concentration of ammonia solution increases to 22%. As shown in Figure 1(b), the volume of a-GA-10% is about 1.81 cm^3 , while it is reduced to 0.61 cm^3 for a-GA-22%. Using the volume of a-GA-10% as a reference, the relative volume of a-GA-22% is shrunk to 33%. The significant shrinkage of GA results in the increase of its density. From Figure 1(b) it could be seen that the density of GA increases from 16.5 mg cm^{-3} to more than 70 mg cm^{-3} when the ammonia concentration increases from 10% to 22%. The increase of the density and the decrease of the volume after ammonia solution treatment indicates the strong coalescent of graphene sheets, which could lead to the enhanced mechanical strength of GA. As shown in Figure 1(c), the compressive strength of a-GA-N improves slightly when it is treated by ammonia solution with lower concentration, while it reaches as high as 2.1 kPa for a-GA-22%.

As reported previously, when GH was directly dried at room temperature, GA with high compressive strength could be obtained since GH shrank seriously. However, the porous structure of GH was lost³⁴. In the present study the ammonia solution treatment not only improves the mechanical strength of GA without sacrificing its porous structure, but also controls its density by adjusting the concentration of ammonia solution. It is well known that when GHs are soaking in ammonia solution, the water inside the system is partially replaced by ammonia solution until the concentration goes to balance. Consequently, when the GH is treated by ammonia solution



with higher concentration, the resulting ammonia concentration contained in the GH should increase, which therefore leads to higher ice point³⁵. During the freeze drying process, ammonia volatilizes gradually, and water inside the GHs evaporates simultaneously until the solution is frozen. The shrinkage of GH is accompanied by the evaporation of water; therefore, the shrinkage of GH could be controlled by adjusting the evaporation time of water (which is controlled by the concentration of ammonia solution inside the GH), then GAs with controllable volume or density can be obtained by the controllable shrinkage of GHs.

It is interesting that not only the porous structure is maintained, but also the macroscopic radial structure is obtained after ammonia solution treatment, as observed from the SEM images of the samples. From the SEM images with low magnification shown in Figure 2(a–d), it can be seen that all the samples possess radial structure. When the concentration of the ammonia solution is low, graphene sheets are interlaced together to form porous structure. When the ammonia concentration is increased to 22%, graphene sheets tend to form tightly layered architecture. Details of the porous structures are shown in Figure 2(e–h). There are abundant macropores in the samples, which decrease significantly in sizes when the samples are treated by the ammonia solution with high concentration. Correspondingly, the macropore walls become thicker, especially for *a*-GA-22%. Although the macropores decrease significantly when the concentration of ammonia solution increases, the specific surface area of all the samples is maintained at about 350 m² g^{−1}, and the N₂ adsorption-desorption isotherm curves (Figure S1) are similar with each other despite of the shrinkage of GH. The developed macropores with high specific surface area and radial structure in GAs make them ideal candidates for adsorption applications. On the contrary, when GH is directly dried at room temperature, the resulting GA will shrink seriously and rare pores can be found. The surface of the GA is tight and smooth (Figure S2), and the specific surface area is only 80 m² g^{−1}.

X-ray photoelectron spectroscopy shown in Figure 3(a) indicates that GA has a predominant graphitic C 1s peak at around 284.6 eV and a weak O 1s peak at around 532 eV, but has no N 1s peak without ammonia solution treatment. When GHs are pretreated by ammonia solution of different concentrations, N 1s peak appears, and the content of N is about 2%, which has little change. Because the ammo-

nia is excessive, there is sufficient ammonia to react with graphene. The increase of ammonia concentration influences little on the reaction between graphene and ammonia. Detailed information can be seen from the C 1s spectra of GA and *a*-GA-N. Besides the typical peaks of GA (C-C/C=C at 284.6 eV, C-O/O-C-O at 286.1 eV, C=O at 287.9 eV and O-C=O at 289.2 eV), there is a new peak for C-N at 285.4 eV observed in the spectrum of *a*-GA-N, indicating that a new covalent C-N bond is formed between graphene nanosheets and ammonia. It is worth noting that the intensities of C-N do not increase significantly with increasing ammonia concentration, indicating that almost all the active sites of graphene sheets could have reacted with ammonia with lower concentration. Moreover, as shown in Figure 3(b–f), the intensities of C-C/C=C peak increase due to hydrothermal processing and ammonia soaking, indicating that GO is partially reduced to form GA, and GA is further reduced by ammonia to form *a*-GA-N.

3D GA materials have been considered as ideal adsorbents for water purification^{4,36}. Because of its high specific surface area and abundant functional groups, GO could theoretically adsorb Pb²⁺ as high as 842 mg g^{−1} at 293K³⁷. But it is hard to remove from water due to its excellent hydrophilic property. Alternatively, *a*-GA-N could be more suitable for water purifying because of its high specific surface area, radial structure, high mechanical strength and easy separation. Here, we test the adsorption capacity of *a*-GA-N towards Pb²⁺ in water. As shown in Figure 4(a), the *a*-GA-10% keeps its initial shape after being shaken for 24 h in the Pb²⁺ solution, demonstrating that it has high mechanical strength and can be reclaimed easily. Figure 4(b) shows that *a*-GA-10%, *a*-GA-14% and *a*-GA-18% exhibit similar adsorption capability for Pb²⁺ despite of their significant differences in volume. Their adsorption capability could be as high as 80 mg g^{−1}, which is higher than those of *a*-GA-22% (about 68 mg g^{−1}) and GA (55 mg g^{−1}) and much better than that of activated carbon^{38–40}. That means without sacrificing the adsorption capacity, the volume of *a*-GA-N can be controlled to save space and it is more convenient and efficient to remove some pollutants out of water. If their adsorption capacities are calculated by volume, the *a*-GA-22% could at least adsorb as much as 5000 g Pb²⁺ per cubic meter as shown in Figure 4(c), which is 5 times more than that of GA. The results well demonstrate that the samples are convenient and effective in water purification. The possible reason for the high adsorption capacity of

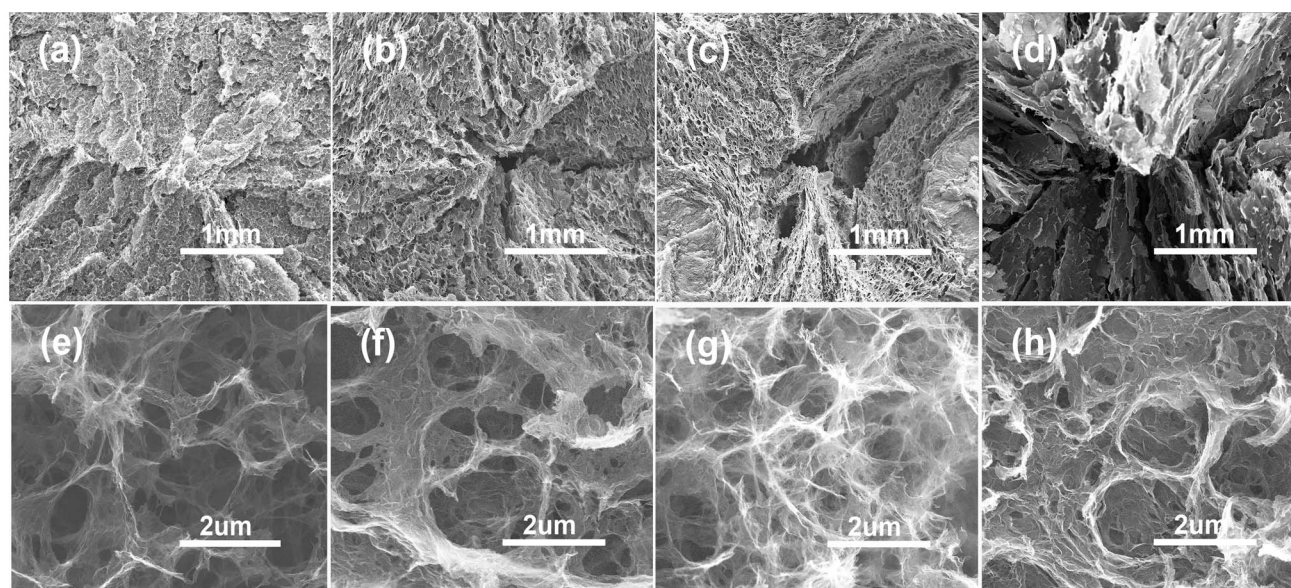


Figure 2 | SEM images of *a*-GA-N. Low and high magnification SEM images of *a*-GA-10% (a and e), *a*-GA-14% (b and f), *a*-GA-18% (c and g) and *a*-GA-22% (d and h) indicate that the macropores of *a*-GA-N are less when they are treated by ammonia solution with higher concentration, while the pore walls become thicker.

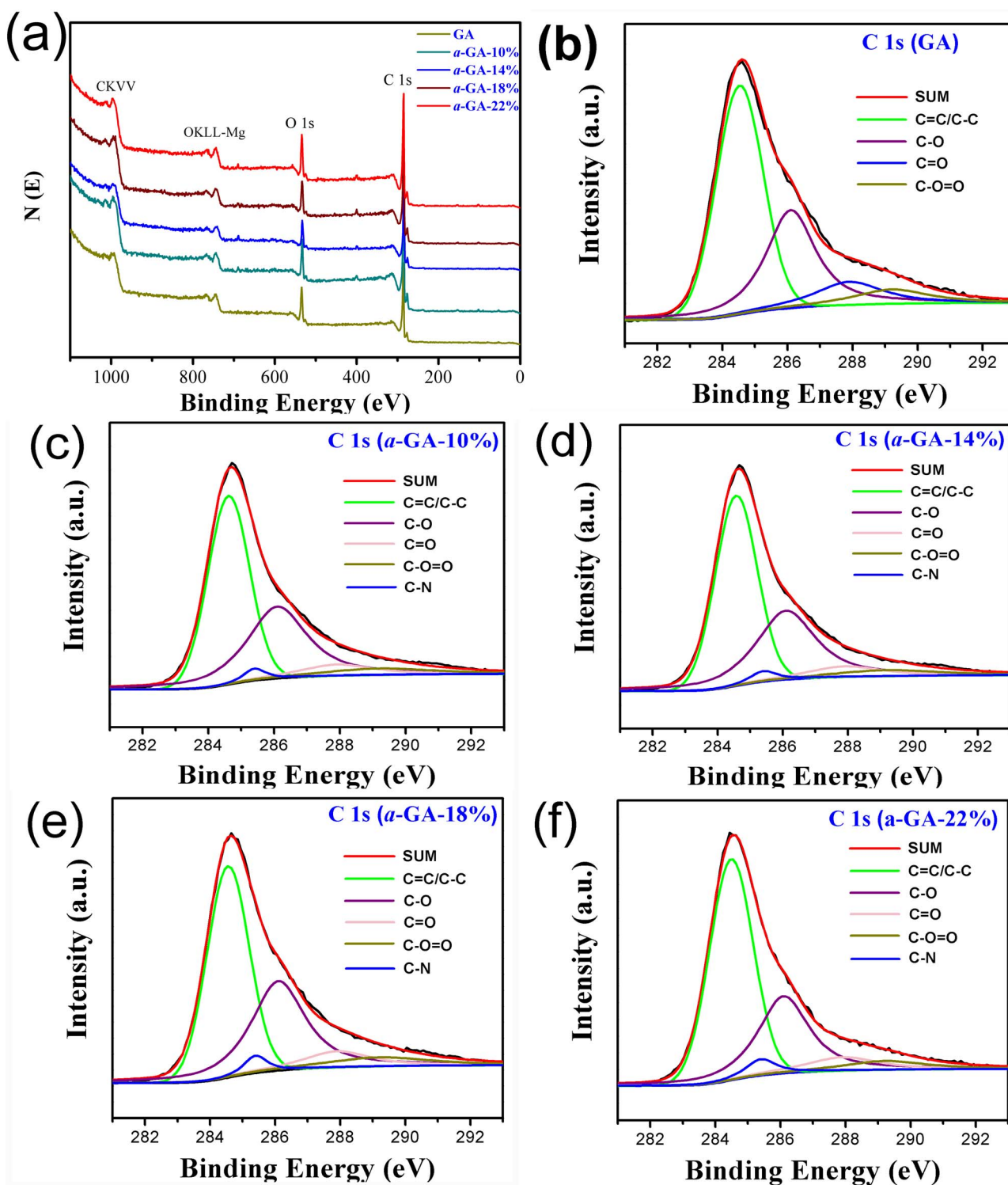


Figure 3 | (a) X-ray photoelectron spectra of GA and a-GA-N, and the corresponding C 1s spectra of GA (b), a-GA-10% (c), a-GA-14% (d), a-GA-18% (e), and a-GA-22% (f).

a-GA-N could be the increased adsorption active sites due to the existence of N covalent bonds. The slight decrease in the Pb^{2+} adsorption capacity of a-GA-22% may be attributed to the serious reduction in its macropores. It is noted that the adsorption reaches equilibrium in about 2 hrs, which is much faster than that of activated carbon⁴¹. This phenomenon is attributed to its unique porous and macroscopic radial structure. Furthermore, after directly separated from the polluted solution, GA could be regenerated via an ion desorption process, the adsorption capability of the regenerated a-

GA-10% still reaches 52 mg g^{-1} in the 5th cycle, as shown in Figure S3, which is 65% of its maximum adsorption capacity.

The interaction between the samples and Pb^{2+} is detected by differential pulse anodic stripping voltammetry (DPASV). As shown in Figure 5, the anodic peak observed at about -0.53 V is fitted into the redox reaction of Pb^{2+} deposition, and the peak intensities represents the mass of lead ions adsorbed by GA or a-GA-10%. The results demonstrate that the intensity of a-GA-10% is slightly higher than that of GA. As is just reported⁴², slight N-doping of graphene could

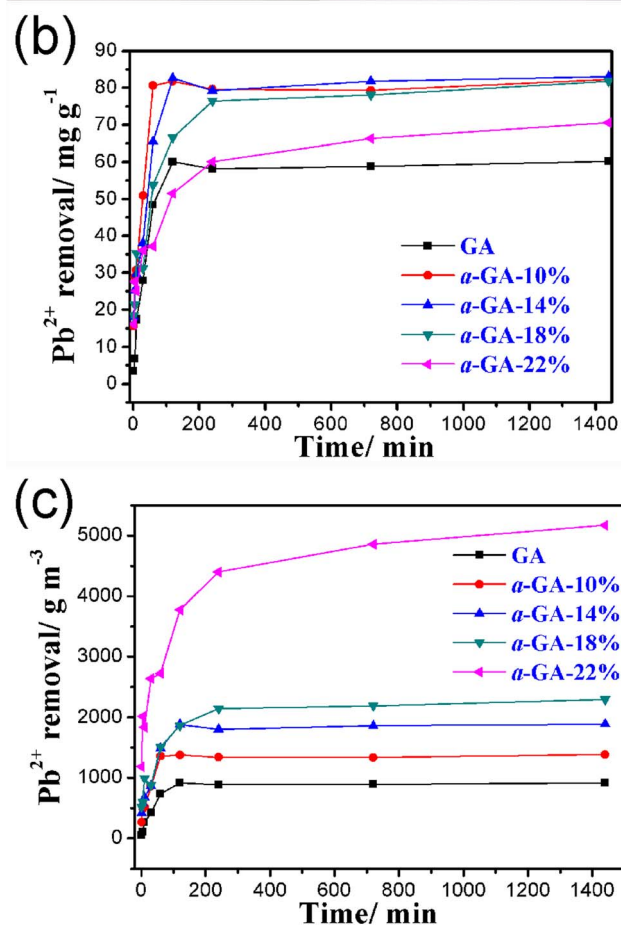
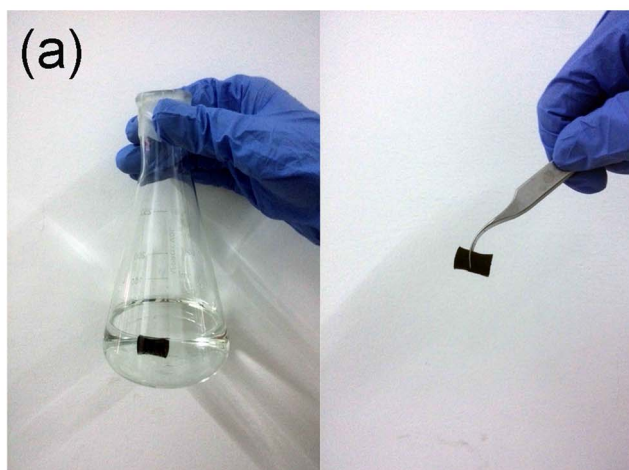


Figure 4 | (a) Photograph of a-GA-N after Pb^{2+} adsorption under shaking condition for 24 h. The well-defined cylinder shape is maintained because of its excellent mechanical strength. (b) Kinetics of Pb^{2+} adsorption of GA and a-GA-N. (c) Adsorption capacity by volume of GA and a-GA-N. The adsorption capacity of a-GA-22% could reach as high as over 5000 $g\ m^{-3}$.

improve its affinities to Pb^{2+} , indicating that nitrogen introduced onto graphene sheets could play an important role in the adsorption of Pb^{2+} because of its lone-paired electrons.

Besides the excellent adsorption capability for Pb^{2+} , a-GA-N also demonstrates high adsorption capacity for organic solvents. Figure S4(a) shows that a-GA-10% can adsorb toluene as high as 41 times of its own weight. When the volume of a-GA-N is reduced, as shown in Figure S4(b), the adsorption capability for toluene decreases, suggest-

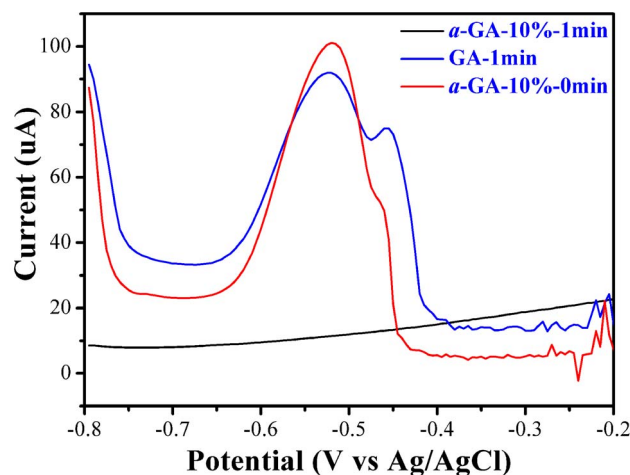


Figure 5 | Differential pulse anodic stripping voltammetric curves of Pb^{2+} .

ing that the adsorption capability for organic solvents is mainly affected by the porosity.

Conclusion

GAs with high mechanical strength, tunable volume and density were prepared. Mechanical strength of GA was enhanced significantly when the hydrogel was soaked in ammonia solution with high concentration. Although the macropores of GAs decreased resulting from the volume shrinkage of GHs, the specific surface area was maintained at about $350\ m^2\ g^{-1}$, and the radial structure appeared after ammonia solution treatment. Because of their unique structure and high specific surface area, GAs prepared in this work demonstrated high adsorption ability for Pb^{2+} and organic solvents. The advantages and potential applications of GAs are significant. For example, they can be used as environmentally friendly materials for waste water treatment and energy conversion and storage.

Methods

Synthesis of samples. Graphene oxide was chemically exfoliated via a modified Hummer's method⁴³ from natural graphite flakes. The details were described in the supplementary information. GO solution of $2\ mg\ ml^{-1}$ was prepared by the sonication of 2.2 g graphite oxide in 1 L water for about 2 hrs, after which the aggregates were removed by mild centrifugation (3000 rpm for 10 mins). Graphene hydrogels (GHs) were fabricated by a typical hydrothermal method. In brief, 35 ml ($2\ mg\ ml^{-1}$) of GO solution was put in a Teflon-lined stainless-steel autoclave, sealed, and hydrothermally treated at $180^\circ C$ for 20 hrs to obtain GH. The obtained GH was put into another stainless-steel autoclave, which was hydrothermally treated by 35 ml of ammonia solution with varying concentration (10%, 12%, 14%, 16%, 18%, 20% and 22% (the original ammonia solution was considered 28v/v%)) at $90^\circ C$ for 1 hr. Then GH was transferred to a freeze dryer directly after the vessel was cooled to room temperature. After freeze drying for 72 hrs at $-70^\circ C$, the strengthened and volume controllable GA was obtained. The GHs after ammonia treatment were labelled as a-GH-N, which were further labelled as a-GA-N after freeze drying, where N referred to the concentration of ammonia. As comparison, the GH without ammonia solution treatment was directly freeze dried with the same condition, which was denoted as GA.

Characterization. Mechanical strength of the samples was measured by a compression testing machine (Materials Testing Machine, ZWICK). The morphology and structure of a-GA-N were observed by field emission scanning electron microscopy (FESEM, FEI Quanta FEG) with an accelerating voltage of 20 kV. Functional groups and chemical bonds of samples were determined by X-ray photoelectron spectroscopy (XPS, PHI 5000C ESCA) at a base pressure of 1×10^{-9} mbar. Specific surface areas of the samples were measured by nitrogen adsorption-desorption isotherms performed at 77 K on a Micromeritics ASAP-2020 volumetric adsorption system, and the specific surface area (SSA) was calculated by the Brunauer-Emmett-Teller (BET) method.

Pb^{2+} adsorption experiments were carried out at room temperature. Typically, GA or a-GA-N (30.0 mg) was put into 100 ml aqueous solutions with Pb^{2+} concentration of $100\ mg\ l^{-1}$, then which was shaken for different durations. After adsorption, the a-GA-N and GA were directly removed from the solution. The



concentration of metal ions after adsorption was determined by atomic absorption spectrophotometer (ASS, TA5-990). The adsorption capacities of the adsorbents were calculated by the formula

$$Q_e = (C_0 - C_f)V/M,$$

Where C_0 and C_f represent the initial and final concentrations (mg g^{-1}), respectively, and V is the volume of the solutions (ml); M is the mass of the adsorbents (mg). The adsorption/desorption performance were also measured. The samples after Pb^{2+} adsorption were treated by dilute nitric acid (0.1 M) at 90°C for 1 hr to remove the adsorbed Pb^{2+} , then the samples were washed by distilled water to neutral, after dried at 100°C for 6 hrs, the samples were allowed to adsorb Pb^{2+} again with the same procedure as the first adsorption, the process was repeated for five times. The interaction between the samples and Pb^{2+} was investigated by an electrochemical workstation (CHI760D, CH Instrument) using a three-electrode cell. In the three-electrode system, Pt was the counter electrode; Ag/AgCl was the reference electrode; a glassy carbon (GC) of 3.0 mm in diameter coated with the sample acted as the working electrode. Details of the characterization were described in the supplementary information.

- Novoselov, K. S. *et al.* A roadmap for graphene. *Nature* **490**, 192–200 (2012).
- Huang, X., Qi, X., Boey, F. & Zhang, H. Graphene-based composites. *Chem. Soc. Rev.* **41**, 666–686 (2012).
- Chua, C. K. & Pumera, M. Chemical reduction of graphene oxide: a synthetic chemistry viewpoint. *Chem. Soc. Rev.* **43**, 291–312 (2014).
- Nardocchia, S. *et al.* Three dimensional macroporous architectures and aerogels built of carbon nanotubes and/or graphene: synthesis and applications. *Chem. Soc. Rev.* **42**, 794–830 (2013).
- Zhang, L. *et al.* Porous 3D graphene-based bulk materials with exceptional high surface area and excellent conductivity for supercapacitors. *Sci. Rep.* **3**, 1408 (2013).
- Gong, Y. *et al.* Graphene-Network-Backboned Architectures for High-Performance Lithium Storage. *Adv. Mater.* **25**, 3979–3984 (2013).
- Zhang, X., Li, Z., Liu, K. & Jiang, L. Bioinspired Multifunctional Foam with Self-Cleaning and Oil/Water Separation. *Adv. Funct. Mater.* **23**, 2881–2886 (2013).
- Qiu, L. *et al.* Biomimetic superelastic graphene-based cellular monoliths. *Nat. Commun.* **3**, 1241 (2012).
- Li, N. *et al.* Three-dimensional graphene foam as a biocompatible and conductive scaffold for neural stem cells. *Sci. Rep.* **3**, 1604 (2013).
- Wu, T. *et al.* Three-dimensional graphene-based aerogels prepared by a self-assembly process and its excellent catalytic and absorbing performance. *J. Mater. Chem. A* **1**, 7612 (2013).
- Gao, H. *et al.* Mussel-inspired synthesis of polydopamine-functionalized graphene hydrogel as reusable adsorbents for water purification. *ACS Appl. Mater. & Interf.* **5**, 425–432 (2013).
- Zhang, L. *et al.* Three-dimensional assemblies of graphene prepared by a novel chemical reduction-induced self-assembly method. *Nanoscale* **4**, 7038–7045 (2012).
- Cui, S. *et al.* Controllable synthesis of silver nanoparticle-decorated reduced graphene oxide hybrids for ammonia detection. *The Analyst* **138**, 2877–2882 (2013).
- Chen, W. & Yan, L. In situ self-assembly of mild chemical reduction graphene for three-dimensional architectures. *Nanoscale* **3**, 3132–3137 (2011).
- Ai, W. *et al.* Formation of graphene oxide gel via the π -stacked supramolecular self-assembly. *RSC Adv.* **2**, 12204 (2012).
- Xu, Y., Sheng, K., Li, C. & Shi, G. Self-Assembled Graphene Hydrogel via a One-Step Hydrothermal Process. *ACS Nano* **4**, 4324–4330 (2010).
- Moon, G. H. *et al.* Catalytic templating approaches for three-dimensional hollow carbon/graphene oxide nano-architectures. *Nanoscale*, **5**, 6291–6296 (2013).
- Zheng, Q. *et al.* Transparent Conductive Films Consisting of Ultralarge Graphene Sheets Produced by Langmuir–Blodgett Assembly. *ACS Nano* **5**, 6039–6051 (2011).
- Yin, S. *et al.* Functional Free-Standing Graphene Honeycomb Films. *Adv. Funct. Mater.* **23**, 2972–2978 (2013).
- Chen, Z. *et al.* Three-dimensional flexible and conductive interconnected graphene networks grown by chemical vapour deposition. *Nat. Mater.* **10**, 424–428 (2011).
- Biener, J. *et al.* Macroscopic 3D nanographene with dynamically tunable bulk properties. *Adv. Mater.* **24**, 5083–5087 (2012).
- Choi, B. G. *et al.* 3D Macroporous Graphene Frameworks for Supercapacitors with High Energy and Power Densities. *ACS Nano* **6**, 4020–4028 (2012).
- Hu, H. *et al.* Ultralight and Highly Compressible Graphene Aerogels. *Adv. Mater.* **25**, 2219–2223 (2013).
- Zhao, Y. *et al.* A Versatile, Ultralight, Nitrogen-Doped Graphene Framework. *Angew. Chem. Int. Ed.* **124**, 11533–11537 (2012).
- Sun, H., Xu, Z. & Gao, C. Multifunctional, ultra-flyweight, synergistically assembled carbon aerogels. *Adv. Mater.* **25**, 2554–2560 (2013).
- Tang, Z., Shen, S., Zhuang, J. & Wang, X. Noble-metal-promoted three-dimensional macroassembly of single-layered graphene oxide. *Angew. Chem. Int. Ed.* **49**, 4603–4607 (2010).
- Zhao, S. *et al.* Three dimensional N-doped graphene/PtRu nanoparticle hybrids as high performance anode for direct methanol fuel cells. *J. Mater. Chem. A* **2**, 3719–3724 (2014).
- Cong, H.-P., Ren, X.-C., Wang, P. & Yu, S.-H. Macroscopic Multifunctional Graphene-Based Hydrogels and Aerogels by a Metal Ion Induced Self-Assembly Process. *ACS Nano* **6**, 2693–2703 (2012).
- Zhang, J., Yu, Y., Liu, L. & Wu, Y. Graphene-hollow PPy sphere 3D-nanoarchitecture with enhanced electrochemical performance. *Nanoscale* **5**, 3052–3057 (2013).
- Wu, Z.-S. *et al.* Three-Dimensional Nitrogen and Boron Co-doped Graphene for High-Performance All-Solid-State Supercapacitors. *Adv. Mater.* **24**, 5130–5135 (2012).
- Wu, Z.-S. *et al.* 3D Nitrogen-Doped Graphene Aerogel-Supported Fe_3O_4 Nanoparticles as Efficient Electrocatalysts for the Oxygen Reduction Reaction. *J. Am. Chem. Soc.* **134**, 9082–9085 (2012).
- Xiao, L. *et al.* Self-Assembled Fe_2O_3 /Graphene Aerogel with High Lithium Storage Performance. *ACS Appl. Mater. & Interf.* **5**, 3764–3769 (2013).
- Han, Z. *et al.* Ammonia solution strengthened three-dimensional macro-porous graphene aerogel. *Nanoscale* **5**, 5462–5467 (2013).
- Bi, H. *et al.* Low temperature casting of graphene with high compressive strength. *Adv. Mater.* **24**, 5124–5129 (2012).
- Elliott, L. D. The Freezing Point Curve of the System Water-Ammonia. *J. Phys. Chem.* **28**, 887–888 (1923).
- Deng, X., Lu, L., Li, H. & Luo, F. The adsorption properties of Pb(II) and Cd(II) on functionalized graphene prepared by electrolysis method. *J. Hazard. Mater.* **183**, 923–930 (2010).
- Zhao, G. *et al.* Removal of Pb(II) ions from aqueous solutions on few-layered graphene oxide nanosheets. *Dalton Trans.* **40**, 10945–10952 (2011).
- Zhang, Y. *et al.* Adsorption of nitrate ions onto activated carbon prepared from rice husk by NaOH activation. *Desalin Water Treat.* **1**–7 (2013).
- Saleh, T. A., Gupta, V. K. & Al-Saadi, A. A. Adsorption of lead ions from aqueous solution using porous carbon derived from rubber tires: Experimental and computational study. *J. Colloid Interf. Sci.* **396**, 264–269 (2013).
- Bouhamed, F., Elouear, Z., Bouzid, J. & Ouddane, B. Batch sorption of Pb(II) ions from aqueous solutions using activated carbon prepared from date stones: equilibrium, kinetic, and thermodynamic studies. *Desalin Water Treat.* **1**–11 (2013).
- Sontheimer, H., Crittenden, J. & Summers, R. *Activated carbon for water treatment*. (Universitaet Karlsruhe, 1988).
- Wang, B. *et al.* Exploring the Interaction between Graphene Derivatives and Metal Ions as a Key Step towards Graphene-Inorganic Nanohybrids. *Chem. Asian J.* **8**, 410–413 (2013).
- Hummers, W. S. & Offeman, R. E. Preparation of Graphitic Oxide. *J. Am. Chem. Soc.* **80**, 1339–1339 (1958).

Acknowledgments

We acknowledge the financial support of National Nature Science Foundation of China (51102168, 51102169, 51272157, 51202147), Shanghai Nature Science Foundation (11ZR1424700), Innovation Program of Shanghai Municipal Education Commission (12YZ093), The Innovation Fund Project For Graduate Student of Shanghai (JWCXSL1401), the Science and Technology Innovation Commission of Shenzhen, and the Program for Eastern Scholar at Shanghai Institutions of Higher Learning.

Author contributions

Z.T., Z.H. and J.Y. designed the experiments, analyzed the data and prepared the manuscript. Z.H. and Z.T. conducted the experiments. S.S. and B.Z. supported discussed the interpretation of results. All authors discussed the results and commented on the manuscript.

Additional information

Supplementary information accompanies this paper at <http://www.nature.com/scientificreports>

Competing financial interests: The authors declare no competing financial interests.

How to cite this article: Han, Z. *et al.* Strengthening of Graphene Aerogels with Tunable Density and High Adsorption Capacity towards Pb^{2+} . *Sci. Rep.* **4**, 5025; DOI:10.1038/srep05025 (2014).



This work is licensed under a Creative Commons Attribution-NonCommercial-NoDerivs 3.0 Unported License. The images in this article are included in the article's Creative Commons license, unless indicated otherwise in the image credit; if the image is not included under the Creative Commons license, users will need to obtain permission from the license holder in order to reproduce the image. To view a copy of this license, visit <http://creativecommons.org/licenses/by-nc-nd/3.0/>